Friction drilling of cast metals

Scott F. Miller, Jia Tao, Albert J. Shih*

Department of Mechanical Engineering, University of Michigan, Ann Arbor, MI 48109-2125, USA

Abstract

This study investigates the friction drilling process, a nontraditional hole-making technique, for cast metals. In friction drilling, a rotating conical tool is applied to penetrate work-material and create a bushing in a single step without generating chip. The cast aluminum and magnesium alloys, two materials studied, are brittle compared to the ductile metal workpiece material used in previous friction drilling research. The technical challenge is to generate a cylindrical shaped bushing without significant radial fracture or petal formation. Two ideas of pre-heating the workpiece and high speed friction drilling are proposed. Effects of workpiece temperature, spindle speed, and feed rate on experimentally measured thrust force, torque, and bushing shape were analyzed. The thrust force and torque decreased and the bushing shape was improved with increased workpiece temperature. Varying spindle speed shows mixed results in bushing formation of two different work-materials. The energy, average power, and peak power required for friction drilling were calculated and analyzed to demonstrate quantitatively the benefits of workpiece pre-heating and high spindle speed in friction drilling.
© 2005 Elsevier Ltd. All rights reserved.

Keywords: Friction; Drilling; Cast metals; Chipless hole making

1. Introduction

Friction drilling is a nontraditional hole-making method that utilizes the heat generated from friction between a rotating conical tool and the workpiece to soften and penetrate the work-material and generate a hole in a thin-walled workpiece [1–4]. Friction drilling is also called thermal drilling, flow drilling, form drilling, or friction stir drilling. It forms a bushing in-situ from the thin-walled workpiece and is a clean, chipless process. The purpose of the bushing is to increase thickness for threading and available clamp load. Ref. [1] has reviewed the technology and principles of the friction drilling process. The process is typically applied to ductile sheet metal, but there is a lack of research in friction drilling of brittle cast metals.

For brittle cast metals, the bushing generated by friction drilling exhibits cracks or petal formation. This problem is illustrated in Figs. 1 and 2. For brittle metals, the deformation of material and petal formation, i.e., fracture in the bushing or lip, is similar to that in the plate perforation or hole flanging using a conical tool [5,6]. Petal formation generates a bushing with limited surface area and load carrying capability for thread fastening.

Figs. 1(a) and (b) illustrate stages in friction drilling of brittle and ductile metal workpiece, respectively. First, the tool comes into initial contact with the workpiece. Next, at the main thrust stage, the tool penetrates the workpiece and a high axial force is encountered. The friction force on the contact surface produces heat and softens the work-material. Then, in the material separation stage, the tool penetrates through the workpiece and makes a hole. The difference in the brittle and ductile workpiece can be seen as the brittle work-material begins to fracture (Fig. 1(a)) and the ductile work-material encompasses the tool (Fig. 1(b)). Finally, the tool retracts and leaves a hole with a bushing on the workpiece. Pictures of friction drilled bushing using a 5.3 mm diameter carbide tool on the brittle cast aluminum 380 alloy, denoted as Al380 hereafter, and the ductile cold-rolled AISI 1020 carbon steel are shown in Figs. 2(a) and (b), respectively, for comparison. For Al380, due to the fracture or peeling in the bushing forming process during friction drilling, much of the work-material is improperly displaced and does not form a bushing with

---

*Corresponding author. Tel.: +1 734 647 1766; fax: +1 734 936 0363.
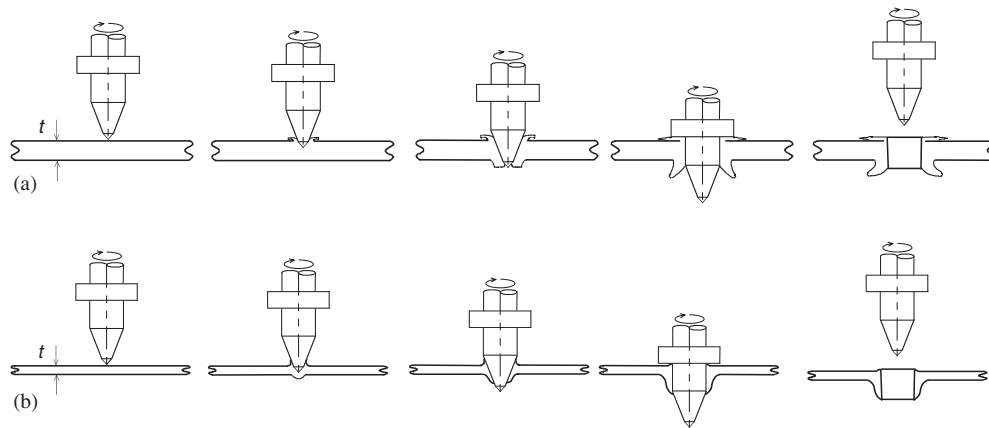 E-mail address: shiha@umich.edu (A.J. Shih).

Fig. 1. Comparison of friction drilling steps in (a) brittle cast metal and (b) ductile sheet metal.
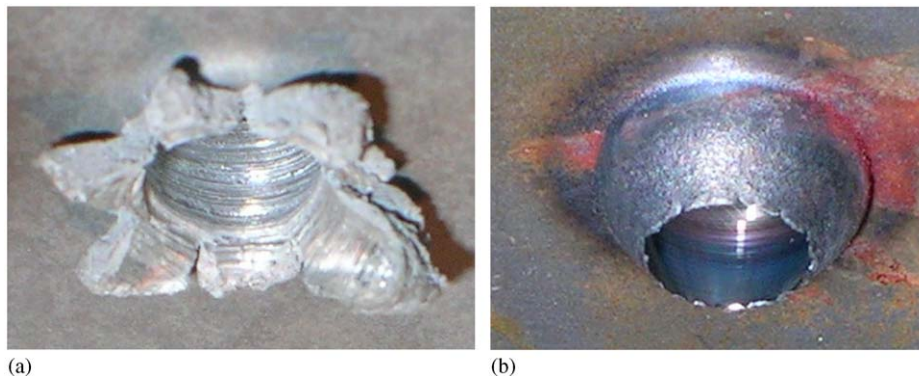

Fig. 2. Bushing of friction drilled hole using 5.3 mm diameter tool: (a) cast Al380 at 5500 rpm with petal formation and bushing fracture and (b) AISI 1020 carbon steel at 2500 rpm.

the desired shape or added thickness to the hole for threading. In comparison, the AISI 1020 workpiece in Fig. 2(b) has a smooth, cylindrical bushing shape with sufficient length.

Cast metals are widely used for industrial, particularly automotive, applications. Ideally, the friction drilling process can generate a hole in the casting. The self-threading fastener [7] can then be applied to join other devices to the casting using friction drilled holes. This approach can simplify the casting mold design and the subsequent assembly process. The goal of this research is to overcome the poor bushing shape due to the material fracture in friction drilling.

The ratio of workpiece thickness, t, to tool diameter, d, is an important parameter in friction drilling. The t and d are marked in Figs. 1 and 3, respectively. A high t/d represents that a relatively larger portion of material is displaced and contributed to the bushing forming. In this experiment for cast metals, the t/d is 0.75. This is high compared to the 0.16 of the AISI 1020 steel in [1].

The experimental setup and procedure are first introduced in this paper. Thrust force and torque for friction drilling experiments are analyzed. The energy, average power, and peak power required to drill each hole are

calculated and analyzed. Finally, the bushing shape and quality are observed and evaluated.

2. Experimental setup and procedure

A Mori-Seiki TV-30 CNC vertical machining center was used for the friction drilling of Al380 with workpiece pre-heating. For high spindle speed test, a Milacron Saber CNC vertical machining center was used. The drilling setups in both machines were the same. Overview of the setup in Mori-Seiki TV-30 is shown in Fig. 4. The workpiece was held in a vise on top of a Kistler model 9272A piezoelectric drilling dynamometer, used to measure the axial thrust force and torque during drilling. The tool was held by a standard collet tool holder. Fig. 3 shows key dimensions of a friction drilling tool. The tool used in this study has $d = 5.3$ mm, $\alpha = 90°$, $\beta = 36°$, $h_c = 0.940$ mm, $h_n = 5.518$ mm, and $h_l = 7.043$ mm. The tool material is tungsten carbide and titanium carbide in cobalt matrix.

Two materials used for experiments in this friction drilling study were 4.0 mm thick die cast Al380 and magnesium AZ91D alloy, denoted as MgAZ91D. Al380 is the aluminum–silicon–copper alloy. MgAZ91D is a light-weight magnesium–aluminum–zinc alloy. Table 1 shows

material properties of these materials relevant to friction drilling, compared to properties for AISI 1020 steel, which is used in the previous friction drilling tests in [1]. Materials with higher strength should require more thrust force to be penetrated. Elongation at break is an indicator of the work-material machinability and can be correlated to the quality of bushing. The low elongation at break of cast
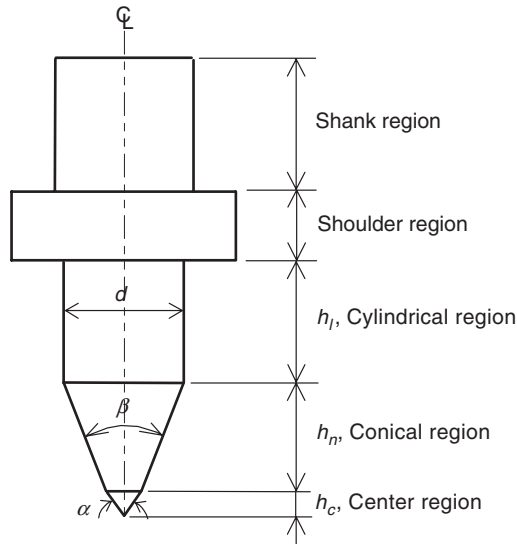

Fig. 3. Key dimensions of the friction drilling tool.

metals suggests the high likelihood of fracture and petal formation. Thermal properties provide information on how the work-material responds to the frictional heating at tool-workpiece interface. The heat transfers away from the interface region quickly for high thermal conductivity workpiece, which, in turn, reduces the workpiece temperature and ductility for bushing formation. Melting temperature of the workpiece material is also important. The maximum temperature generated in friction drilling was noticed to be about 1/2 to 2/3 of the workpiece melting temperature [1].

Two ideas, the pre-heating of workpiece to elevated temperature and the high spindle speed friction drilling, were hypothesized. It is well known that at elevated temperature the cast metal has increased plasticity, which can make the work-material conform to the tool and less likely to fracture during friction drilling. For magnesium alloy, the exothermic oxidation at elevated temperature is a problem. The cast MgAZ91D ignited inside the oven during heating. Therefore, friction drilling of MgAZ91D at elevated temperature was not performed in this study. In another effort to increase the temperature and plasticity in work-material, high spindle speed tests, greater than 5500 rpm, were conducted for both materials. It has been shown in friction stir welding that more heat is generated at higher rotational speed of the tool [8,9]. The effect of spindle speed in friction drilling is studied.
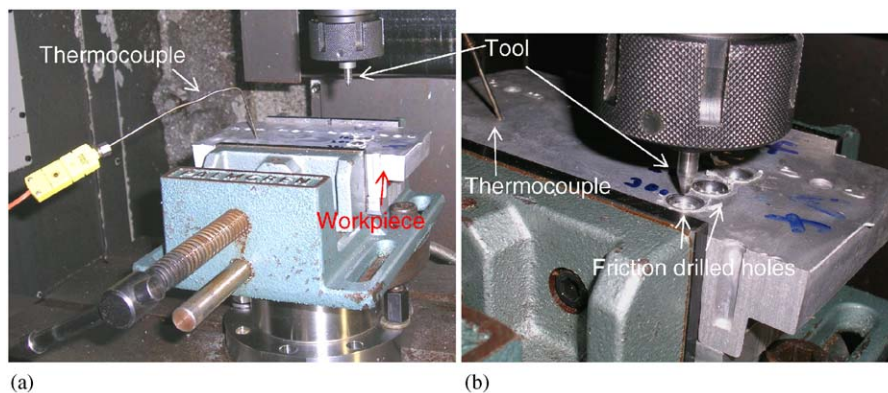

Fig. 4. Experimental setup with tool, workpiece, vise, thermocouple, and drilled holes: (a) overview and (b) close-up view.

Table 1
Comparison of material properties [11,12]

	Al380	MgAZ91D	AISI 1020 carbon steel, cold rolled
Density (kg/m^3)	2710	1810	7870
Hardness, Brinell (kgf/mm^2)	80	63	121
Elongation at break (%)	3	3	15
Ultimate tensile strength (MPa)	330	230	420
Tensile yield strength (MPa)	165	150	350
Modulus of elasticity (GPa)	71	45	205
Thermal conductivity (W/mK)	96.2	72.0	51.9
Melting point (°C)	540–595	470–595	1430

Table 2
Test matrix for friction drilling of heated workpiece and high spindle speed tests

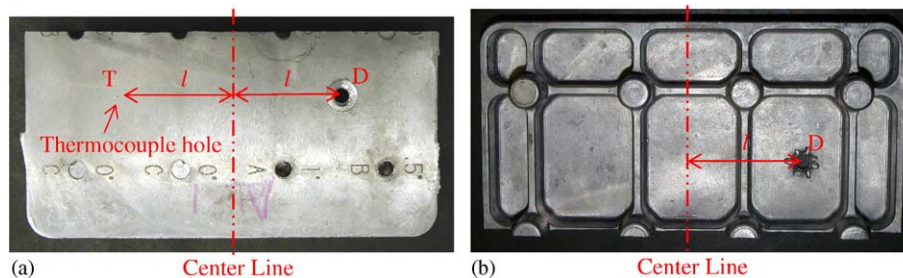| Exp.	Work material	Feed rate (mm/min)	Spindle speed (rpm)	Workpiece temperature (°C)
I	Al380	254	5500	300
				200
				100
				25 (room)
II	Al380	305	5500	300
				200
				100
III	Al380	356	5500	300
				200
IV	Al380	406	5500	300
V	Al380	254	3000	25 (room)
			7000	
			11000	
			15000	
VI	MgAZ91D	254	3000	25 (room)
			7000	
			11000	
			15000	

Fig. 5. Symmetric shape of the Al380 workpiece: (a) top view and (b) bottom view.

Table 2 shows the test matrix. Four sets of experiment, marked as Exps. I–IV, were conducted to study the effect of workpiece temperature and feed rate on friction drilling of Al380. The spindle speed remained constant at 5500 rpm. The highest workpiece temperature of Al380 was limited to 300 °C. Above this temperature, severe surface oxidization and bubble formation were observed in the workpiece. At 300 °C, the highest feed rate at 406 mm/min was utilized in Exp. IV. The feed rate was varied according to workpiece temperature as described in Table 2.

To achieve the elevated temperature in Exps. I–IV, the Al380 workpiece was first heated in an oven to slightly beyond 300 °C. The workpiece was then removed from the oven and placed in the vise. Then, as shown in Fig. 4, a contact thermocouple (Omega Model KMQIN-062G-6) with 1.5 mm diameter was placed in a small hole on the workpiece to predict the temperature at the friction drilling spot, which is symmetric to the thermocouple location on the workpiece. The thermocouple reading was monitored as the workpiece cooled. As the temperature at the drilling

spot cooled down and reached the targeted 300, 200, and 100 °C values, a hole was drilled. During drilling, the time to penetrate a hole at the lowest feed rate was less than 3 s. Therefore, the workpiece temperature drop by natural convection during the 3 s was not significant, even at the high workpiece temperature of 300 °C.

The workpiece used in this study, as shown by the top and bottom views in Fig. 5, has a symmetrical shape relative to the center line. Temperatures at two points, marked as T and D in Fig. 5, should be about the same, assuming the thermal transport in the workpiece is symmetric relative to the center line. Point T is the thermocouple location for temperature measurement. Point D is the center of the friction drilled hole. These two points have the same distance, l, to the center line, as shown in Fig. 5. Therefore, the temperature at location D was assumed to be the same as that measured by the thermocouple at location T.

High spindle speed drilling tests, Exp. V for Al380 and Exp. VI for MgAZ91D, were performed at room temperature workpiece under the same feed rate of 254 mm/min.

Four spindle speeds experimented were 3000, 7000, 11000, and 15000 rpm.

For every test in Exps. I–VI, the thrust force and torque were measured and bushing quality was examined. The sampling rate was 750 samples per second. The measured data was filtered using a moving average.

3. Thrust force and torque

The measured thrust force and torque of Exps. I–IV for friction drilling of Al380 at 25, 100, 200, and 300 °C are shown in Fig. 6. The horizontal axis represents the time and distance of tool travel from the initial contact between tool and workpiece. The time to penetrate the workpiece varies depending on the feed rate. The shape of the thrust force vs. time is different from that of the high and narrow peak at the start of contact in friction drilling of steel sheet metal as presented in [1]. For friction drilling of cast metal with high t/d, the thrust force increases at a slower rate to a

peak value, about 3 mm tool travel from the start of contact. At this tool location, the frictional heating becomes more effective to raise the workpiece temperature and soften the work-material (4 mm thick). From the peak, the thrust force reduces at an almost constant rate until the tool penetrates the workpiece and the thrust force reaches a value close to zero.

The general trend for torque, which rises and falls at a slow rate, is different from that of thrust force but similar to that of torque in friction drilling of AISI 1020 steel [1]. The contact area on the periphery of the tool determines the torque, which usually peaks after the tool has penetrated the workpiece [1]. As shown in Fig. 6, the peak of torque occurs at about 6–8 mm from the start of contact, much later than the peak of thrust force. The distance of tool travel to generate a hole with a bushing is about 11 mm from the start of contact.

The benefit of high feed rate to reduce cycle time in friction hole drilling of pre-heated workpiece is demonstrated.
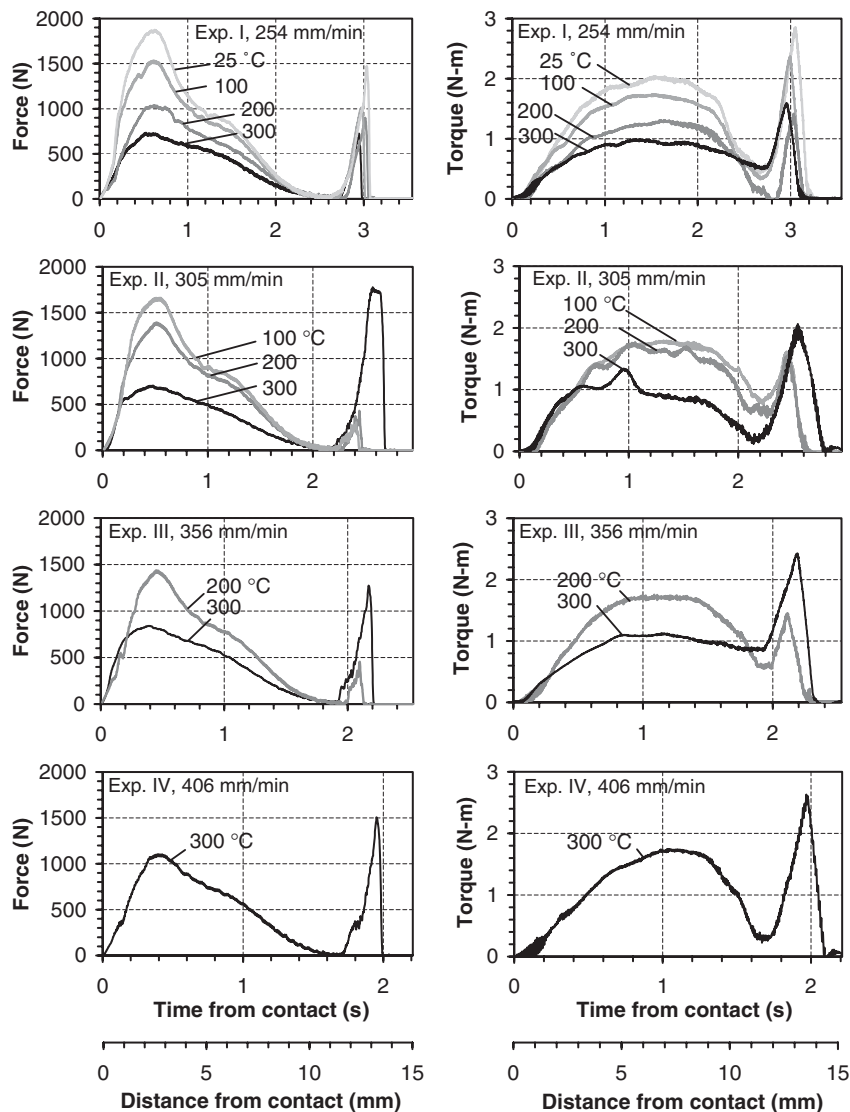

Fig. 6. Thrust force and torque in friction drilling of cast Al380 workpiece at 5500 rpm in Exps. I–IV.
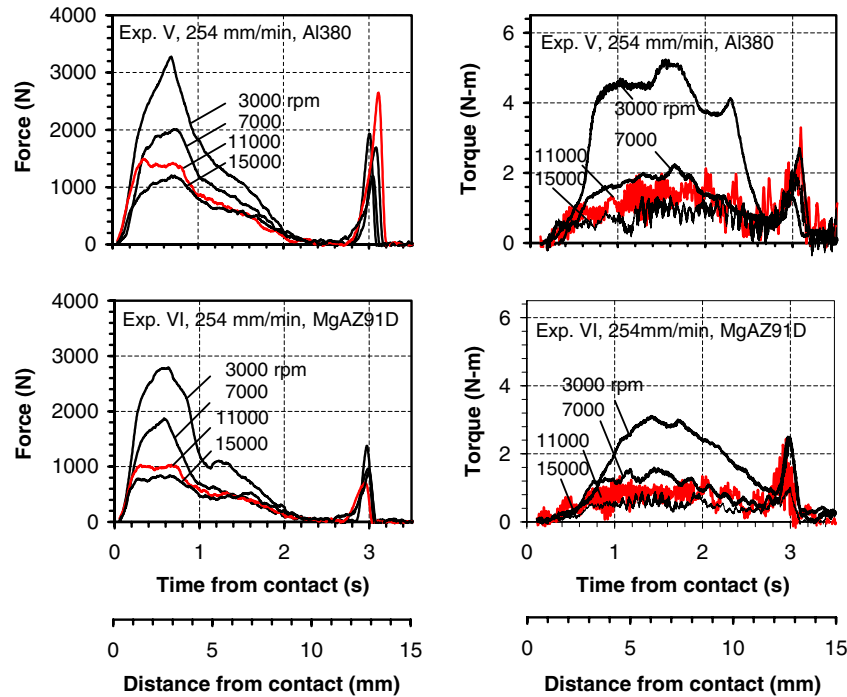
Fig. 7. Spindle speed effect on the thrust force and torque in friction drilling at 254 mm/min feed rate in Exps. V and VI.

For the 254, 305, 356, and 406 mm/min feed rate, the time for hole generation is about 2.5, 2.0, 1.8, and 1.6 s, respectively.

In Fig. 6 secondary peaks in thrust force and torque can be seen. After penetration, the shoulder of the tool, which is marked in Fig. 3, contacted the back-extruded work-material. It pushed in and flattened the face of the workpiece, as shown later in the cross-section view of drilled holes. The contact of tool shoulder and workpiece created the secondary peak of thrust force and torque after the tool penetration of workpiece. Fig. 6 shows that peak values of this thrust force and torque could be large, even higher than the thrust force and torque in penetration, due to the large shoulder area of the tool used in this study. If a tool without shoulder is used, no secondary peak of the thrust force and torque is expected. In this case, a small bushing will be formed by the back extrusion of the work-material at the entry of the friction drilled hole.

Effects of workpiece temperature and feed rate on peak thrust force and torque were analyzed. In Exp. I, at 25, 100, 200, and 300 °C workpiece temperatures, the peak thrust forces are 1900, 1500, 1000, and 700 N and the torques are 2.0, 1.7, 1.3, and 1.0 N-m, respectively. The benefit of high workpiece temperature to reduce the thrust force and torque is identified. Lower peak forces and torques mean that higher feed rate can be applied at high workpiece temperature. From Exps. I to IV, under the same 300 °C workpiece temperature, the feed rate of 254, 305, 356, and 406 mm/min generate peak thrust force of 700, 700, 800, and 1100 N and peak torque of 1.0, 1.4, 1.2, and 1.7 N-m, respectively. The rapid increases of thrust force and torque

show the limitation of high feed rate in practical friction drilling of a pre-heated workpiece.

Large variation of the recorded torque trace was noticed. This is due to the material adhesion from the Al380 workpiece to the tool. Aluminum is known to have a high affinity for the tool [10]. A layer of build-up aluminum alloy transferred to the tool surface. Filing and sanding processes were applied to clean the tool after each hole was drilled to remove the build-up work-material and to ensure the consistent tool surface quality and repeatable thrust force and torque measurements. The tool tip is usually clean without the adhesion of work-material. The low surface speed at the tool tip indicates that the speed and temperature are key factors in the adhesion of aluminum alloy on the tool surface. This observation suggests further investigations of material transfer and adhesion and possibly of using a tool coating to alleviate this problem.

The effect of spindle speed on the thrust force and torque in friction drilling of room temperature Al380 and MgAZ91D under the same feed rate, 254 mm/min, is shown in Fig. 7. At 3000, 7000, 11000, and 15000 rpm spindle speeds, the peak thrust forces are 3300, 2000, 1500, and 1200 N for Al380 and 2700, 1800, 1000, and 800 N for MgAZ91D, respectively. All tests show the MgAZ91D has slightly lower peak thrust force than that of Al380. At the low, 3000 rpm, spindle speed the thrust force and torque are very high. High peak torque of Al380 and MgAZ91D at 5 and 3 N-m, respectively, can be seen at 3000 rpm. Benefits of decreasing thrust force and torque from 3000 to 7000 rpm spindle speed are very obvious. This demonstrates a threshold tool speed for

friction drilling. In Section 4, the energy and power for friction drilling can further validate this observation quantitatively. The increased spindle speed reduces the torques to about 1–2 Nm and 0.5–1.5 N-m for Al380 and MgAZ91D, respectively. High variation of torque at high spindle speeds can be observed. This is due to the adhesion of work-materials to the tool at high speed.

4. Energy and power in friction drilling

The analysis of power and energy in friction drilling provides the basic information for the machine requirements, such as the selection of the spindle and design of the fixture for workholding. Most of the energy converts into heat and transfers to the workpiece and tool.

Over the time from the start of tool-workpiece contact to penetration of the hole, the energy E required for friction drilling can be expressed as:

$$E = \int_0^{\Delta t} Fv\,dt + \int_0^{\Delta t} T\omega\,dt, \qquad (1)$$

where Δt is the time duration of drilling, F the thrust force, v the tool axial velocity, t the time, T the torque, and ω is the tool rotational speed. The rotational motion contributes to nearly all, over 99%, of the energy consumed in friction drilling.

The average power required to generate a hole by friction drilling is P_{av}:

$$P_{av} = E/\Delta t. \qquad (2)$$

The maximum power delivered in the friction drilling process is P_{max}:

$$P_{max} = T_{max}\omega, \qquad (3)$$

where T_{max} is maximum torque. This is assuming that the force term contributing to the maximum power is comparatively small and neglected.

By analyzing the measured thrust force and toque, E, P_{av}, and P_{max} for each drilling condition can be analyzed.
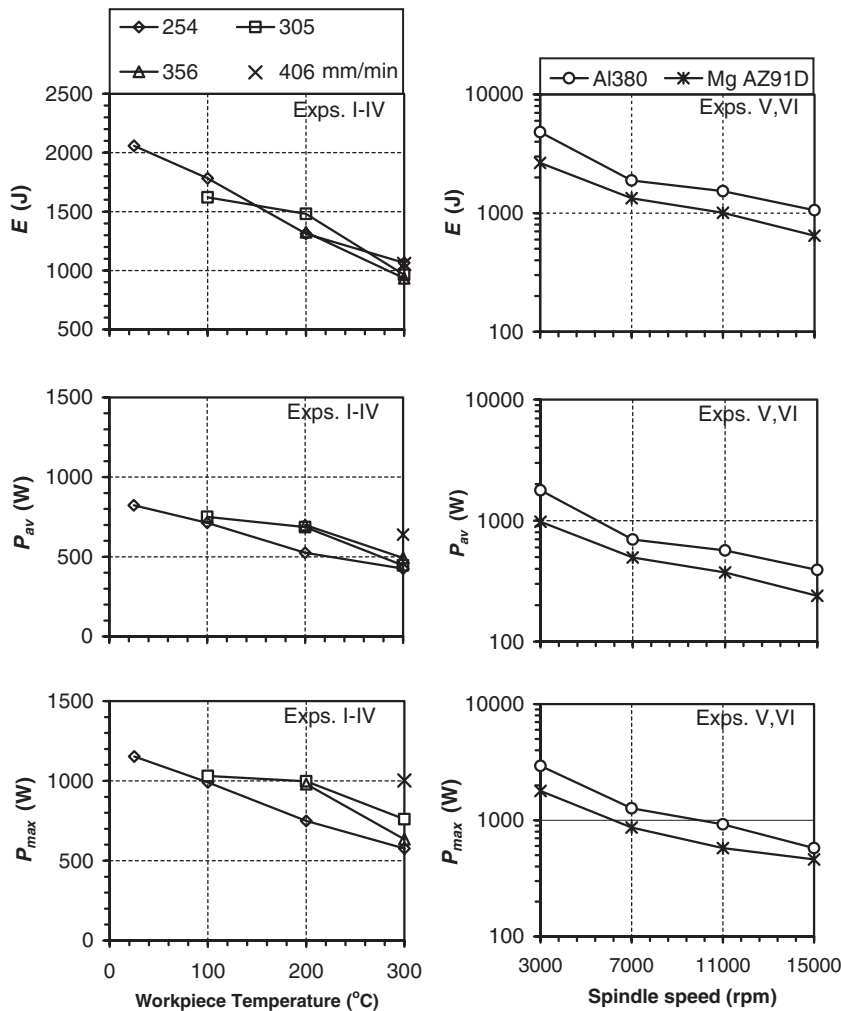

Fig. 8. Energy and average and peak power in friction drilling, 5500 constant rpm spindle speed in Exps. I–IV and 254 mm/min feed rate in Exps. V and VI.

4.1. Energy, E

The top row in Fig. 8 shows the energy E vs. workpiece temperature and spindle speed for friction drilling. In Exps. I–IV, four sets of data points for energy basically overlap each other. This indicates that the energy required to drill a hole is independent of the feed rate. The workpiece temperature has a significant effect on the energy. As the temperature increased from 25 to 300 °C, the energy is reduced in an almost linear trend from 2000 to 1000 J. The high temperature softens the work-material and reduces the energy required for hole drilling.

Results of Exps. V and VI reveal effects of spindle speed and type of work-material. For both Al380 and MgAZ91D, high spindle speed reduces the energy for friction drilling. Consistently, MgAZ91D requires lower energy than Al380. An exponentially decaying E vs. spindle speed is observed, as illustrated in the almost linear trend line of log-scale E vs. spindle speed for both work-materials. Friction hole drilling has to have a sufficiently high spindle speed to make the process effective. Higher spindle speed generates more heat in the tool–workpiece interface, which locally increases the workpiece temperature and enables the effective hole penetration. By increasing the speed from 3000 to 7000 rpm, the energy per hole is reduced from 5200 to 2000 J for Al380. The same significant drop of energy can also be observed in MgAZ91D. In the high spindle speed range, the increase in spindle speed has less noteworthy impact of the energy reduction.

4.2. Average power, P_{av}

The second row in Fig. 8 shows the average power P_{av} for friction drilling. Unlike the energy, the feed rate has some effect on P_{av}. Under the same workpiece temperature, lower feed rate has lower P_{av}. The workpiece temperature also has the close to linear effect on the reduction of average power required for hole drilling. In Exps. I–VI, the highest P_{av}, about 880 W occurs at the lowest workpiece temperature (25 °C) and slowest feed rate (254 mm/min). This is a high but reasonable number for drilling a 5.3 mm diameter hole in Al380. High temperature at 300 °C can help reduce the P_{av} to 480 W. However, at the same 300 °C, P_{av} increased to 700 W for drilling at the highest feed rate (406 mm/min). Since the time duration for hole generation is shorter in hole drilling at high feed rate, the energy per hole is about the same under all four feed rate at 300 °C workpiece temperature.

In Exps. V and VI, the exponentially decaying P_{av} vs. spindle speed can also be observed for both Al380 and MgAZ91D. Mg AZ91D also has smaller P_{av} than Al380.

4.3. Peak power, P_{max}

The peak power P_{max} in friction drilling is illustrated in the bottom row in Fig. 8. The feed rate and workpiece temperature both affect the P_{max}. In general, higher P_{max} was observed at higher feed rate. There are exceptions for 305 and 356 mm/min feed rate. A linear trend of reducing P_{max} vs. workpiece temperature can also be identified.

For Al380 and MgAZ91D, the P_{max} decreases consistently as the spindle speed increases. At the lowest spindle speed (3000 rpm), the peak power of 3000 W is quite high for drilling a 5.3 mm hole in Al380. On the contrary, at 15000 rpm, the peak power is only 570 W for Al380 and 460 W for MgAZ91D.

5. Shape of bushing

The shape of bushing and the depth of the hole are two important but difficult to quantify criteria in evaluating the quality in friction drilling. Qualitative observations of the bushing shape, based on cylindricality, petal formation, thickness, and roughness, were made to judge the success of the friction drilled hole in each case.

5.1. Workpiece heating effect on bushing shape and petal formation

Fig. 9 shows bushing shape from friction drilling of Al380 at different temperatures. Workpiece temperatures in Figs. 9(a)–(d) are 25, 100, 200, and 300 °C, respectively. The view of bushing from bottom of the workpiece and a cross section view of the same hole are shown to reveal and compare different features of the hole and bushing. Petal formation, an undesirable characteristic in friction drilling of cast metals, is marked in Fig. 9(a). These petals, as marked in Fig. 9, were observed to peel from the workpiece in the radial direction. The petal still has the bright, curved surface like the inside of the bushing. This indicates that the petal was part of the bushing during the early stage of friction hole drilling. As the strain in the bushing reaches a critical value, the bushing fractures along the axial direction and bursts into five to eight petals. Four petals bushing can sometimes be observed. The t/d ratio greatly influences the number of petals. Under the small t/d ratio, more petals can be formed in each busing. This has been observed experimentally.

Accompanying the petals are cracks that extend nearly the length of the bushing at the 25 and 100 °C workpiece, as shown in Figs. 9(a) and (b). At 200 °C, as shown in Fig. 9(c), the crack does not extend the whole length of bushing. This shows the petal formation is dependent on the material properties and the benefits of workpiece preheating. At 300 °C, as shown in Fig. 9(d), there is less obvious cracks and petals. The petal formation and cracking are traits of poor bushing formation due to limited ductility of work-material. The petal formation translates to less added thickness for thread on friction drilled holes. Streaks from the tool, as marked in Fig. 9(b),
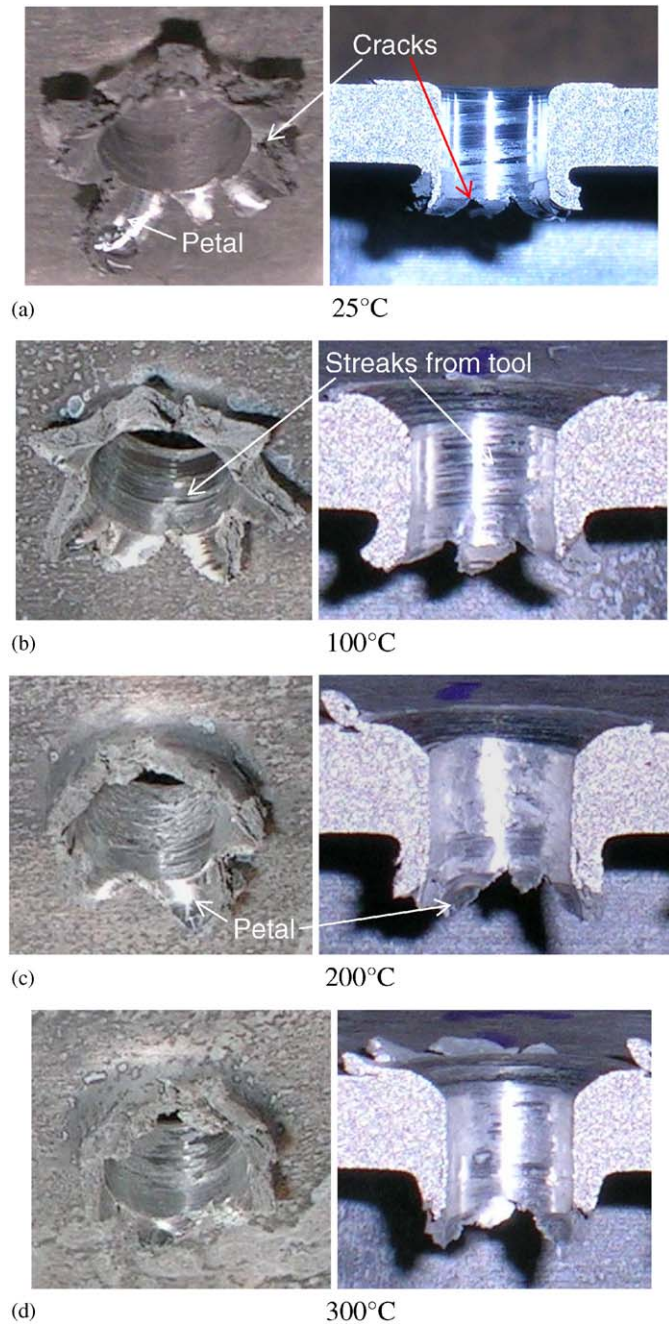
Fig. 9. Bushing formed in friction drilling of Al380 at 254 mm/min feed rate and 5500 rpm spindle speed in Exp. I.

Fig. 10. Bushing and bushing cross section formed in Exps. V and VI.

are an indication of workpiece surface damages and the adhesion of work-material to the tool, as discussed in detail in [2].

As workpiece temperature increases, the bushing formed becomes more cylindrical and has less fracture and radial displacement. This is especially evident in the cross section views. This experiment indicated that drilling at elevated temperature made the workpiece material more ductile and formable, and hence the bushing shape more cylindrical.

No changes in bushing quality were noticed for varying feed rate in the experiment.
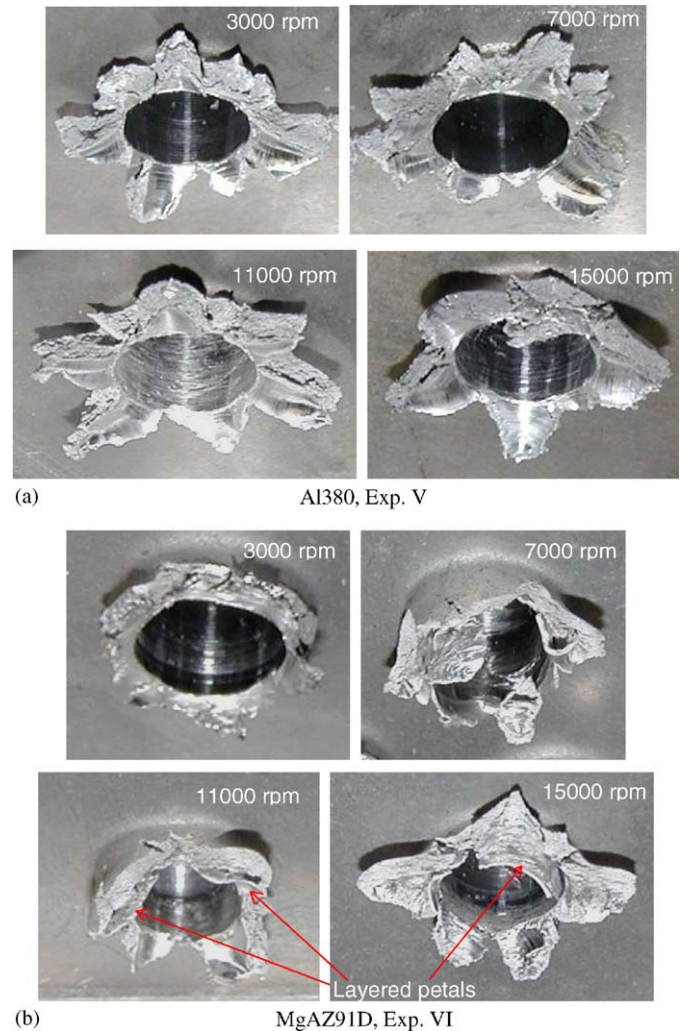
5.2. Spindle speed effect in Al380 and MgAZ91D

Fig. 10 shows the bushing formed in Al380 and MgAZ91D at 3000, 7000, 11000, and 15000 rpm spindle speed. For Al380 at room temperature (no pre-heating the workpiece), as shown in Fig. 10(a), no significant change in bushing shape is noticed by varying the spindle speed. Although the energy and power were reduced at high spindle speed, the bushing shape is still poor at the highest spindle speed. Significant petal formation and cracking are observed in each of the hole. This further distinguished the benefit of workpiece pre-heating to improve the shape of bushing, as discussed in Section 5.1 and shown in Fig. 9.

Spindle speed has a negative effect on the shape of bushing for MgAZ91D. As shown in Fig. 10(b), as the spindle speed increases from 3000 to 15000 rpm, the petal formation becomes more apparent. At 3000 rpm, the shape of bushing is ragged, but no petal formation or peeling is noticed. At 7000 rpm, some but not significant petal formation can be seen in the bushing. At 15000 rpm, very extensive petal formation, similar to the bushing in friction

drilled holes of room temperature Al380, was seen. In addition, the layered petal formation in MgAZ91D, as marked in Fig. 10(b), can be seen. This is likely due to the sliding of a layer of work-material surrounding the tool during the burst of petals.

6. Conclusions

The workpiece pre-heating and high spindle speed had proven to be beneficial to reduce the thrust force, torque, energy, and power for friction drilling of brittle cast metals. Higher feed rate and shorter cycle time for hole drilling was demonstrated to be feasible with the reduced thrust force and torque. For Al380, the shape and quality of bushing were observed to improve at higher workpiece temperature. Less severe cracking and petal formation were observed on bushings formed at elevated workpiece temperature. The high spindle speed did not affect the bushing formation for room temperature Al380. For room temperature MgAZ91D, high spindle speed was detrimental on the bushing shape.

This study has further identified several research topics for friction drilling. The thrust force and torque can be reduced and cycle time can be reduced using the workpiece pre-heating and high spindle speed. New ideas to improve the quality of bushing are still necessary for brittle cast metals. The deformation and fracture of work-material to form petals are not well understood. A finite element model can be used to gain better understanding of the heat transfer and material flow and deformation in friction drilling. Practically, different ways to heat the workpiece, such as using the induction heating to locally raise the temperature on the spot of drilling, need to be developed to implement the proposed technology in friction drilling.

References

[1] S.F. Miller, S.B. McSpadden, H. Wang, R. Li, A.J. Shih, Experimental and numerical analysis of the friction drilling process, ASME Journal of Manufacturing Science and Engineering, 2004, submitted for publication.

[2] S.F. Miller, P. Blau, A.J. Shih, Microstructural alterations associated with friction drilling of steel, aluminum, and titanium, Journal of Materials Engineering and Performance, 2005, accepted for publication.

[3] J.A. van Geffen, Piercing Tools, US Patent 3,939,683, 1976.

[4] J.A. van Geffen, Method and Apparatuses for Forming by Frictional Feat and Pressure Holes Surrounded Each by a Boss in a Metal Plate or the Wall of a Metal Tube, US Patent 4,175,413, 1979.

[5] W.J. Johnson, N.R. Chitkara, A.H. Ibrahim, A.K. Dasgupta, Hole flanging and punching of circular plates with conically headed cylindrical punches, Journal of Strain Analysis 8 (1973) 228–241.

[6] N.M. Wang, M.L. Wenner, An analytical and experimental study of stretch flanging, International Journal of Mechanical Science 16 (1974) 135–143.

[7] D.M. Paxton, M.T. Smith, J.A. Carpenter, P.S. Sklad, Application of thread-forming fasteners (TFFs) in net-shaped holes, FY 2004 Progress Report for Automotive Lightweight Materials, Freedom-CAR and Vehicle Technologies Program, US DOE, 2004, pp. 263–266.

[8] H. Schmidt, J. Hattel, J. Wert, An analytical model for the heat generation in friction stir welding, Modelling and Simulation in Materials Science and Engineering 12 (2004) 143–157.

[9] M. Song, R. Kovacevic, Thermal modeling of friction stir welding in a moving coordinate system and its validation, International Journal of Machine Tools & Manufacturing 43 (2003) 605–615.

[10] N. Sato, O. Terada, H. Suzuki, Adhesion of aluminum to WC-Co cemented carbide tools, Journal of the Japan Society of Powder and Powder Metallurgy 44 (4) (1997) 365–368.

[11] Properties and Selection: Irons, Steels, and High Performance Alloys, 1 (10), Metals Handbook, ASM International, 1990.

[12] Properties and Selection: Nonferrous Alloys and Special-Purpose Materials, 2 (10), Metals Handbook, ASM International, 1990.